processes

MDPI

Article

Molecular Dynamics Study on the Nature of near Miscibility and the Role of Minimum Miscibility Pressure Reducer

Feng Liu [1], Shengbing Zhang [1], Jiale Zhang [1], Zhaolong Liu [1], Yonghui Chen [1] and Shixun Bai [2,*]

[1] Research Institute of Exploration and Development, PetroChina Tuha Oilfield Company, Hami 839009, China; syzxlf@petrochina.com.cn (F.L.); syzxzhsb@petrochina.com.cn (S.Z.); zhangjlkt@petrochina.com.cn (J.Z.); liuzhaolth@petrochina.com.cn (Z.L.); chenyhyjy@petrochina.com.cn (Y.C.)

[2] School of Petroleum, China University of Petroleum-Beijing at Karamay, No. 355, Anding Road, Karamay District, Karamay 834000, China

* Correspondence: baisxun@cupk.edu.cn

Abstract: Gas miscible flooding, especially CO_2 miscible flooding, is a key method for enhanced oil recovery. However, the high Minimum Miscibility Pressure (MMP) often makes true-miscible flooding impractical. A number of studies confirm the existence of a near-miscible region that also ensures high recovery. However, the exact boundary for near miscibility remains unclear, with various speculative definitions based on experimental data or by experience. In this work, a molecular-level understanding of miscibility and near miscibility and the role of the MMP reducer are achieved using the molecular dynamics method. It is found that the traditional criterion of interfacial tension being zero is not valid for the molecular dynamics method, and that the interaction energy between oil molecules suggests distinct boundary between near-miscibility and miscibility regimes. MMP reducers were found to bring the two regions closer in terms of energy, rather than actually reducing the MMP.

Keywords: molecular dynamics; miscibility; near miscibility; MMP reducer

check for updates

Academic Editor: Andrew S. Paluch

Received: 6 January 2025
Revised: 6 February 2025
Accepted: 11 February 2025
Published: 14 February 2025

Citation: Liu, F.; Zhang, S.; Zhang, J.; Liu, Z.; Chen, Y.; Bai, S. Molecular Dynamics Study on the Nature of near Miscibility and the Role of Minimum Miscibility Pressure Reducer. *Processes* **2025**, *13*, 535. https://doi.org/10.3390/pr13020535

Copyright: © 2025 by the authors. Licensee MDPI, Basel, Switzerland. This article is an open access article distributed under the terms and conditions of the Creative Commons Attribution (CC BY) license (https://creativecommons.org/licenses/by/4.0/).

1. Introduction

Gas miscible flooding is one of the most efficient methods for enhanced oil recovery, in which CO_2 miscible flooding plays an essential role [1–3]. A large number of laboratory experiments, theoretical studies, and field trials have been conducted [4–7]. The excessive focus on Minimum Miscibility Pressure (MMP, which refers to the minimum pressure required for the injected gas to achieve multi-contact miscibility with crude oil at the reservoir temperature) has made the ability to achieve miscibility a decisive factor in implementing CO_2 flooding in oil fields. However, due to the sometimes high MMP, true-miscible flooding is not always practical for specific oil fields.

Thomas et al. suggested based on a literature review and field application that the interfacial tension (IFT) between crude oil and injected gas being zero (i.e., miscibility) is not the deciding factor affecting displacement efficiency [8], leading to widespread discussion and attention. Subsequently, researches gradually focused on near-miscible flooding. Orr et al. pointed out that in capillary tube experiments, the recovery curves do not exhibit an abrupt transition from immiscible to miscible states; rather, the region between oil and gas is actually in a state of "near miscibility" [9,10]. Subsequently, Stalkup, Zick, Novosad, and other researchers reanalyzed a large number of field-implemented miscible floods through capillary experiments and equation-of-state calculations, confirming the possibility of a "unconventional miscible flooding" [11–13]. Zick et al. [11] characterized this type of

displacement as having a lower interfacial tension (IFT) between oil and gas phases and a recovery factor higher than 95%. However, they did not specify or quantify how low the IFT should be. Thomas et al. systematically summarized a large amount of field data from miscible floods and suggested that investigations on how to improve gas injection effects at relatively lower pressures (near-miscible flooding) is more practical than actually achieving miscibility [8]. Later, Shyeh-Yung (1991) [14], Crigg (1996) [15], Schechter (1998) [16], and Dong (2000) [17] successively confirmed through long core displacement experiments that there indeed exists a special pressure region near the MMP.

An increasing number of studies have confirmed that near-miscible flooding can achieve development effects comparable to those of miscible flooding [18–21]. Moreover, due to the reduction in injection pressure, the requirements for compressor operating pressure, CO_2 injection volume, and impurity gas content will also be relaxed. However, there is currently no consensus on how to clearly define near miscibility and determine the region of near miscibility. It is mostly vaguely summarized as "some area below MMP" or "close but below MMP". From a physicochemical perspective, miscibility means the disappearance of the oil–gas interface, with an IFT of 0. However, the widely accepted capillary tube experimental method primarily judges whether miscibility is achieved from a recovery perspective. Shyeh-Yung et al. interpreted near-miscible flooding as "a state where the injected gas and oil are not completely miscible but are close to achieving miscibility" [22]. Although Burger, Shen Pingping, and Lars Hoier also noted the existence of near miscibility, they did not explicitly define or delineate this region [23–25]. Huong et al. proposed, based on experience, that the pressure range for CO_2 near-miscible flooding in the Ogallah oil field is (0.8–1) MMP [26]. Mohammad et al. determined through simulation calculations that 83% MMP marks the beginning of near-miscible flooding [27]. It should be noted that these conclusions are mostly speculative based on experimental data or experience, and their accuracy and underlying physical criteria require further verification. Additionally, due to differences in reservoir characteristics, crude oil properties (viscosity, composition, etc.), reservoir temperature, and pressure of the target reservoirs, it remains to be clarified whether it is reasonable to judge whether a target reservoir belongs to near-miscible flooding solely from the perspective of recovery rate or IFT, and what standards should be followed and adhered to for defining the near-miscible boundary. There have been studies that investigated the miscibility of oil and CO_2 [28–32] at molecular scale or pore scale; however, the majority of them are focused on the phase behavior of these fluids within nanopores, which make them more about the distribution of fluid components under confined spaces than about the nature of miscibility. Those that do focus on near miscibility is actually describing miscibility instead [33], or blurring the difference between the two regimes [34]. Therefore, a molecular-level understanding of miscibility and near miscibility is still insufficient.

Apart from accepting near miscibility as a practical substitute, another approach to further relax the requirements for miscibility flooding is to reduce the MMP with chemical additives, that is, MMP reducers [3]. Specifically, surfactants are the most commonly suggested MMP reducers. The mechanisms for their capability to lower the MMP include enhancing the solubilty of CO_2 in oil, facilitating the ability of CO_2 to extract light components from the oil phase, reducing the oil viscosity, lowering the IFT, etc. [3,35–37]. Fluorocarbon and siloxane-based surfactants were shown to be effective in reducing the MMP between CO_2 and oil due to their higher solubility in CO_2 and the high efficiency in lowering the interfacial tension [3,38]. However, fluorocarbon surfactants are highly toxic, while siloxane-based surfactants are prone to hydrolysis and expensive, rendering both types unsuitable for field application [39,40]. Consequently, cost-effective and environmentally friendly hydrocarbon surfactants should be the focus. Therefore, there is a need to

develop new CO_2-philic surfactants to enhance the reduction in the Minimum Miscibility Pressure for CO_2 miscible flooding. Additionally, the molecular-level mechanisms of the role they play in reducing the MMP is still unclear and requires further study.

In this work, the fundamental difference between near miscibility and true miscibility is investigated using molecular dynamics simulations, and the role of MMP reducers is clarified. The rest of the paper is structured as follows. The simulation setup and the model description are first laid out, followed by the analyses on the affinity of CO_2 to different functional groups. Two methods of MMP determination are compared, and the molecular scale boundary between near miscibility and true miscibility is defined. The role of the MMP reducer is explained correspondingly. The results from this work provide deeper understanding of the near-miscibility state and can offer guidance for the MMP reducer design.

2. Methods

2.1. Molecular Dynamics Simulations

The latest version of the GROMACS software at the time of study, GROMACS 2024.1 [41], is used to conduct all simulations in this work because it is extremely fast at calculating the nonbonded interactions [41], which is especially the case for the systems investigated in this study. GROMACS has been widely used for investigations involving polymers and fluid dynamics [42]. The van der Waals interactions are represented by Lennard–Jones potentials with a cut-off distance of 1.2 nm, and the PME (Particle Mesh Ewald) algorithm is used to account for the long-range electrostatic interaction. The time step is set to be 1.0 fs. The simulations are performed at 333 K and a series of pressure conditions under the NPT ensemble, controlled by the c-rescale barostat and the Nosé Hoover thermostat. The CHARMM forcefield [43] is used for the decane molecules which constitute the oil phase, while for CO_2, the EMP2 model [44] is used because it better represents the phase behavior of CO_2.

2.2. Model Description

Figure 1 illustrates the model used to simulate the mixing of decane and CO_2 molecules. A simulation box of 4 nm $\times$ 4 nm $\times$ 122 nm is set, in which 500 decane molecules are inserted as an oil block which is enclosed by 2000 CO_2 molecules on each side. Due to the periodic boundary conditions used along all directions, the system is infinite in the xy plane (parallel to the decane and CO_2 interface). The large size of 122 nm along the z direction is because the gaseous state of the CO_2 molecules, which takes significantly more space compared to the oil phase. The model as shown in Figure 1 represents a binary system with just decane and CO_2, while for simulations with MMP reducers, the reducer molecules are added into the CO_2 phase as the initial configuration. The model system is then subjected to an NPT run, controlled by the Parinello–Rahman barostat, during which the box size changes along the z direction while the x and y dimensions are kept constant depending on the pressure.

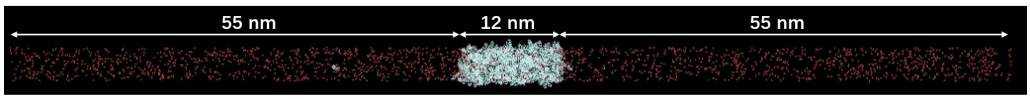


Figure 1. Configuration of the model used to simulate the miscibility of CO_2 and decane oil. An oil block of 12 nm is positioned in the middle of the simulation box, and CO_2 molecules are positioned at both sides of the oil block. Carbon, oxygen, hydrogen atoms are represented by green, red, and white particles, respectively.

2.3. Determination of MMP Using Calculated IFT Method

The interfacial tensions for the decane and CO_2 systems in the absence and presence of MMP reducers are calculated using the method proposed by Zhang et al. [45] as follows:

$$\gamma = \frac{1}{2}\langle h_z(P_n - P_t)\rangle \quad (1)$$

where γ is the interfacial tension, h_z is the length of the simulation box along the z direction, and P_n and P_t are the pressure tensors perpendicular and parallel to the interface.

3. Results and Discussion

3.1. Distribution of CO_2 Around Different Functional Groups

Ketone, ester, ether, and alcohol-type MMP reducers with short carbon chains (to emphasize on the roles of O-containing functional groups) are built as shown in Figure 2, and ten of each type of these molecules are inserted into the simulation boxes filled with CO_2. NPT simulations at 333 K and 6 MPa are run for 20 ns, and the distribution of carbon dioxide molecules around the oxygen atom in the reducers is analyzed. The RDF curves are shown in Figure 3. All RDF curves in this work refer to the variation in number density with the distance from the reference molecule. Since the number density is an absolute value instead of a normalized ratio, all RDF curves and the peaks thereof are inter-comparable. As can be seen in Figure 3, despite the large fluctuations due to the simulations being NPT, which inherently experience large variations in box size, a clear trend can be identified. That is, ketone type attracts the most CO_2 around its oxygen atom, followed by alcohol-type, ester-type, and ether-type reducers. This likely has to do with the partial charges assigned to the oxygen atoms in the forcefield. The oxygen on the ketone-type MMP reducer is sufficiently negative (-0.47) and is only neighbor to one carbon atom on one end, unlike the alcohol, ester, or ether types, which are bonded with either carbon or hydrogen atoms on both ends. This gives room for stronger interaction between the oxygen atoms on the ketone-type MMP reducer and the carbon atom in CO_2. This suggests that molecules containing these types of functional groups (especially ketone groups) and carbon chains of appropriate lengths should be able to facilitate the mingling of CO_2 with the oil phase and contribute to the reduction in the MMP.

In light of the above deduction, a series of MMP reducers with C10 carbon chains and ketone, ether, ester, and alcohol functional groups are constructed and tested in subsequent MD runs (Figure 4). Especially considering the outstanding ability of ketone groups in attracting CO_2 shown in Figure 3, a molecule with five ketone oxygens is built to investigate the impact of ketone group in MMP reduction (Figure 5a). However, during the trial runs, this molecular structure does not exhibit such potentials, as they aggregate into blocks where the molecules are apparently aligned and stay at the CO_2-decane interface without dispersing further into the oil phase (Figure 5). Consequently, no enhanced mixing of CO_2 is obtained as can be proved in the overlapping RDF curves of CO_2 around decane molecules in the presence and absence of the MMP reducer (Figure 6). The reason could be the strong intermolecular interaction between ketone oxygens and ketone carbons which leads to the exceedingly strong conglomeration of these molecules. Similar structures with ether, ester, and alcohol functional groups are no longer investigated in this work; instead, an MMP reducer (C12PO6) structure that is reported to be efficient in MMP reduction in a laboratory study [46] (Figure 7) is chosen together with the structures shown in Figure 4 in subsequent simulations.

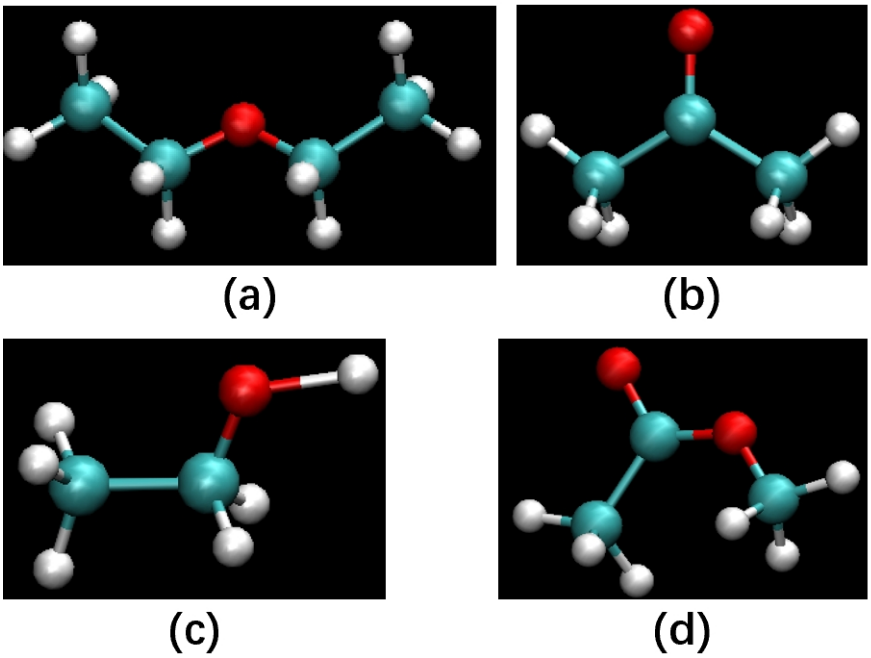


Figure 2. (**a**) Ether-type MMP reducer (diethyl ether), (**b**) ketone-type MMP reducer (ketone), (**c**) alcohol-type MMP reducer (ethanol), and (**d**) ester-type MMP reducer (methyl acetate). All reducers in this figure are deliberately constructed to have short carbon chains to emphasize on the influence of the oxygen atoms on the distribution of CO_2 molecules.

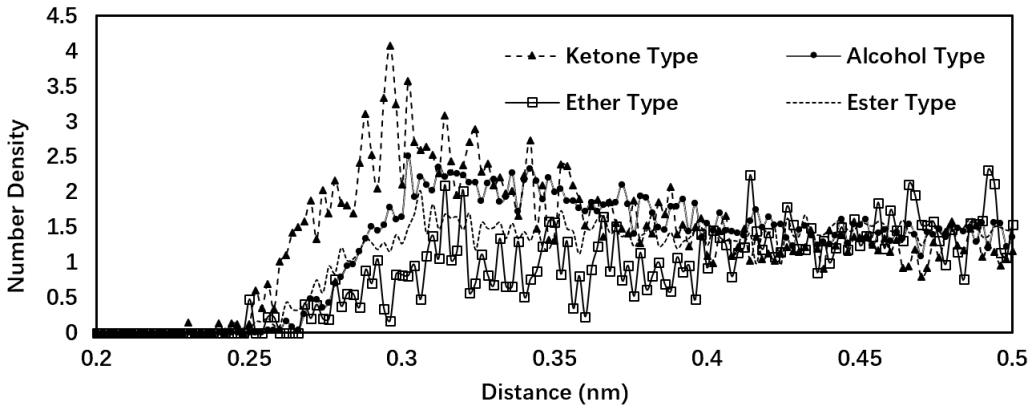


Figure 3. RDF curves of CO_2 molecules around the oxygen atoms in ketone, alcohol, ether, and ester-type MMP reducers.

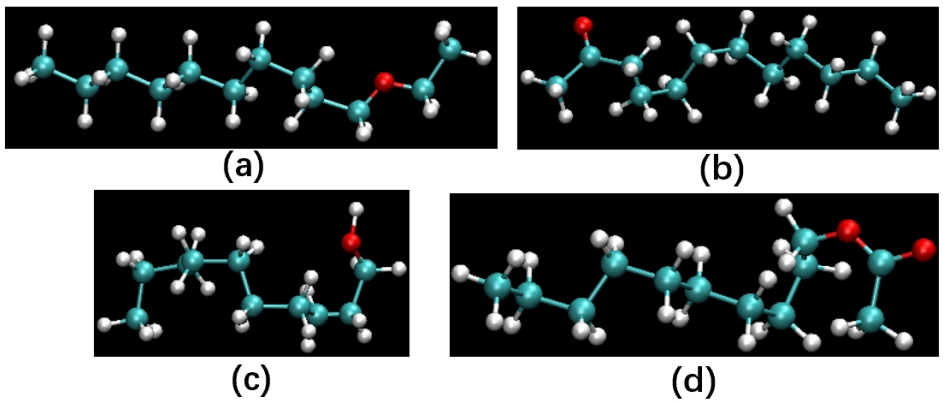


Figure 4. Structures of (**a**) ether-type, (**b**) ketone-type, (**c**) alcohol-type, and (**d**) ester-type MMP reducers with C10 carbon chain.

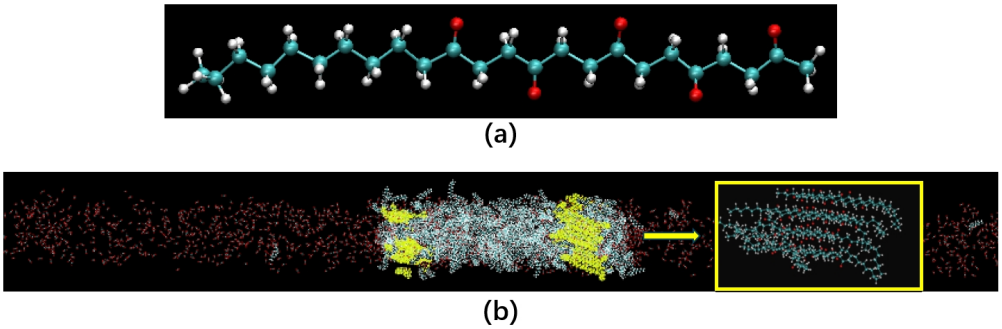


Figure 5. (**a**) Structure of an MMP reducer with 5 ketone groups, (**b**) snapshot of the model system containing 50 of the MMP reducers by the end of 20 ns. The MMP reducers are shown in yellow to better demonstrate their configuration and location.

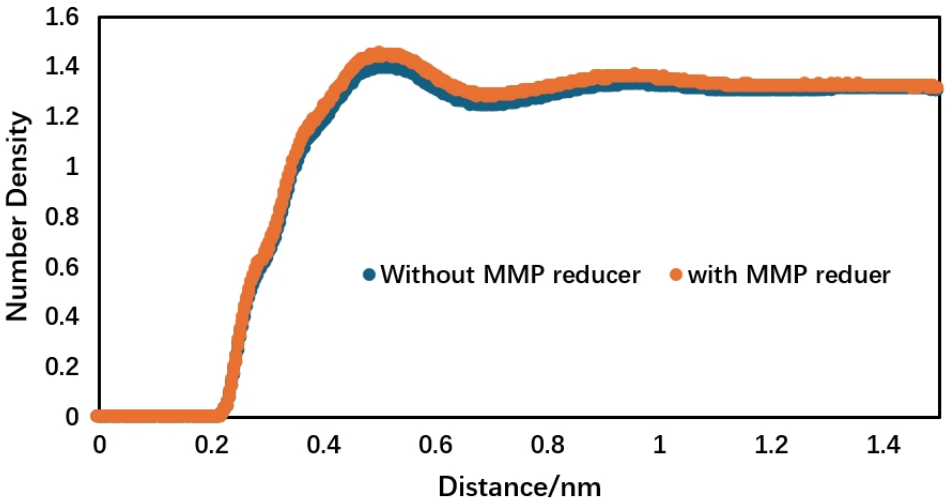


Figure 6. RDF curves of CO_2 around decane molecules in the presence and absence of MMP reducer with five ketone groups.

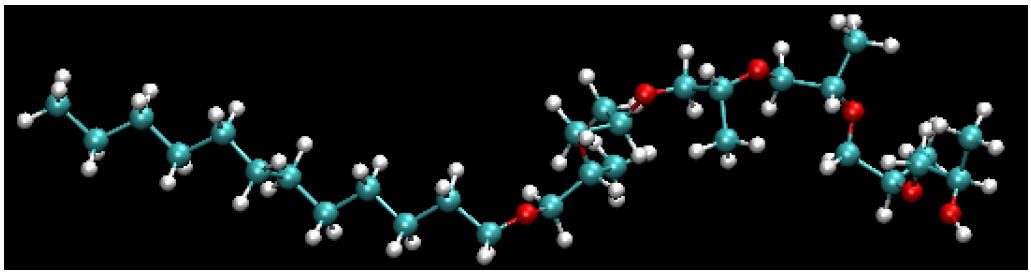


Figure 7. Structure of an MMP reducer C12PO6, with C12 carbon chain and six PO groups.

3.2. Determination of MMP Based on IFT

Using Equation (1), the interfacial tensions between CO_2 and the oil phase are calculated for systems in the presence and absence of various MMP reduces. An example is shown in Figure 8 for the binary system with just decane and CO_2, where the interfacial tension decreases with increasing pressure, and the trend is linearly extrapolated to obtain the X-axis intercept of 10.01 MPa. The value is then considered the MMP for this system at 333 K. Ma [46] reported an MMP of 8.93 MPa at 323 K, and an MMP of 12.15 MPa at 344 K for the decane and CO_2 system. Therefore, our result of 10.01 MPa at 333 K is reasonable and falls in line with the literature.

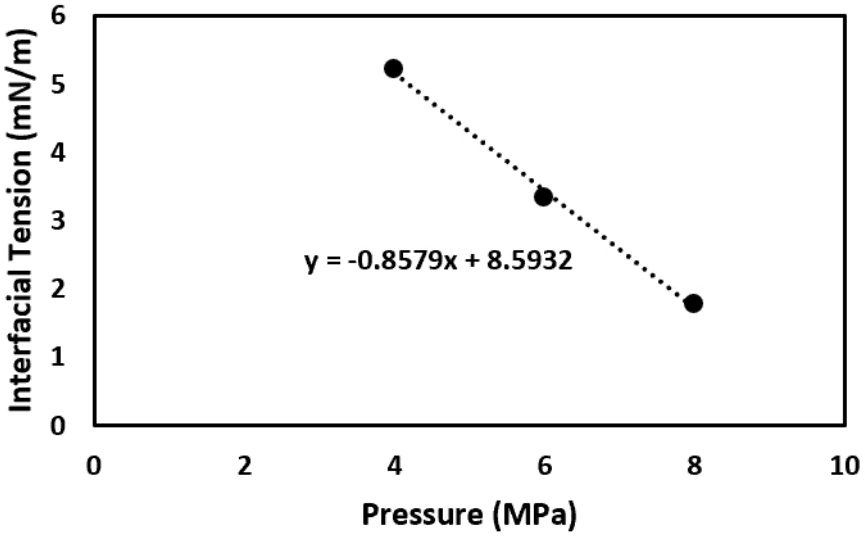


Figure 8. Demonstration of the IFT method, with a trend line fitted onto three interfacial tension values calculated at different pressures and the corresponding equation.

As mentioned earlier, given that the reducers have relatively strong affinity for carbon dioxide molecules, one can expect that these reducers can facilitate the mixing of CO_2 in the oil and therefore lower the MMP. However, although molecular dynamics studies consistently show the lowering of IFT between oil and CO_2 in the presence of surfactants [1–3,35,47], the MMP calculated using the interfacial tension method (Figure 9) suggests that such a trend does not exist. On the contrary, except for the ester-type reducer, all other MMP reducers essentially lead to higher MMPs compared to that for pure CO_2 and decane oil. This is against both the instinct and laboratory evidence. Ma [46] reported a 16% reduction in MMP when using C12PO6 at 344 K, whereas such a trend is not observed in this study using the simulated IFT method, and if anything, the reverse happened. The only rational explanation would be the unsuitability of the method itself in predicting the MMP when surfactants are involved, the major reason again being the lack of a clearly defined interface. Surfactants function by accumulating at the interface, and if no such interfaces exist, its roles are unlikely to be captured and represented by MD-generated IFT values. Deviation of the IFT values from a linear trend at high pressures was reported in an MD study by Wang et al. [3], which they referred to as the second phase. Though no explanations were provided, the existence of such a behavior suggests that in terms of MD studies, the determination of MMP using the IFT method can be inaccurate.

A closer look at the simulation trajectories may indicate the reason. From Figure 10, it can be observed that at lower pressures of 4 MPa, the decane essentially exhibits as a single large cluster, indicating that it is a continuous phase. However, with the gradual increase in pressure, CO_2 easily dissolves in the oil phase, breaking the decane phase into clusters at 8 MPa, indicative of the disappearance of definitive interfaces. With the continual increase in pressure to 16 MPa (Figure 10c), the clusters become smaller and eventually collapse into individual molecules at 20 MPa (Figure 10d). The position of the interfaces are demonstrated in Figure 11. At 4 MPa, although some CO_2 molecules are already dissolved in the decane block, a distinct interface can still be visually identified. As the pressure is increased to 8 MPa, more CO_2 molecules distribute within the oil phase, and the decane block becomes stretched but still has relatively discernable boundaries. The boundaries become completely blurred as the pressure increases to 16 and 20 MPa, when decane and CO_2 clusters are highly mixed throughout the system and an interface entirely disappear. Strictly speaking, during this process, decane is no longer a continuous phase, nor is CO_2.

But for ease of reference, if the clusters of decane molecules that are separated by the dissolved CO_2 can still be considered a phase, then seen from this perspective, interfaces exist in a chaotic arrangement that is difficult to define; therefore, the IFT calculation method is no longer valid in this case. In other words, the exact state of miscibility might be blurred by the high solubility of carbon dioxide in oil. This may explain the failure of MMP prediction using the IFT method. In order to more accurately and reasonably predict the MMP values in MD studies, one has to resort to a different criterion.

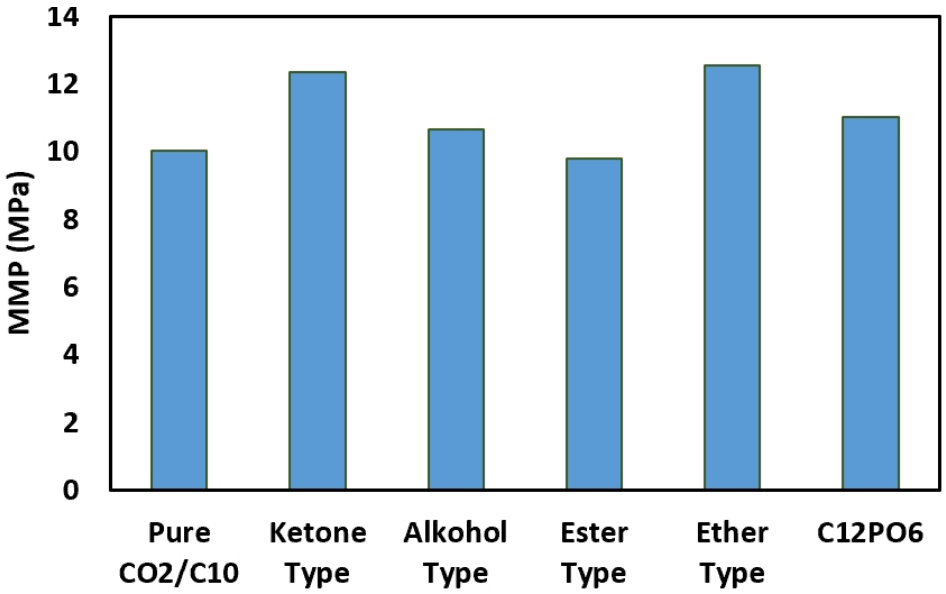


Figure 9. MMP values obtained using the IFT approach for systems without the MMP reducer and ketone-type, alcohol-type, ester-type, and ether-type reducers with C10 chain length, and C12PO6 MMP reducer.

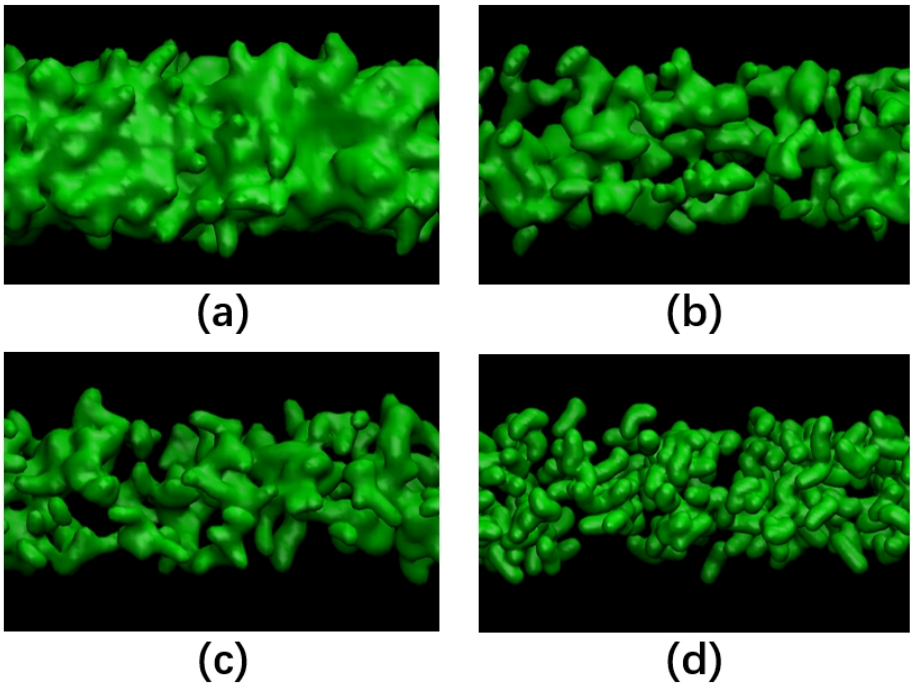


Figure 10. Demonstration of decane clusters at (**a**) 4 MPa, (**b**) 8 MPa, (**c**) 16 MPa, and (**d**) 20 MPa. Clusters of decane molecules are colored in green. The CO_2 molecules occupy the vacant spaces between clusters and are not shown for clarity.

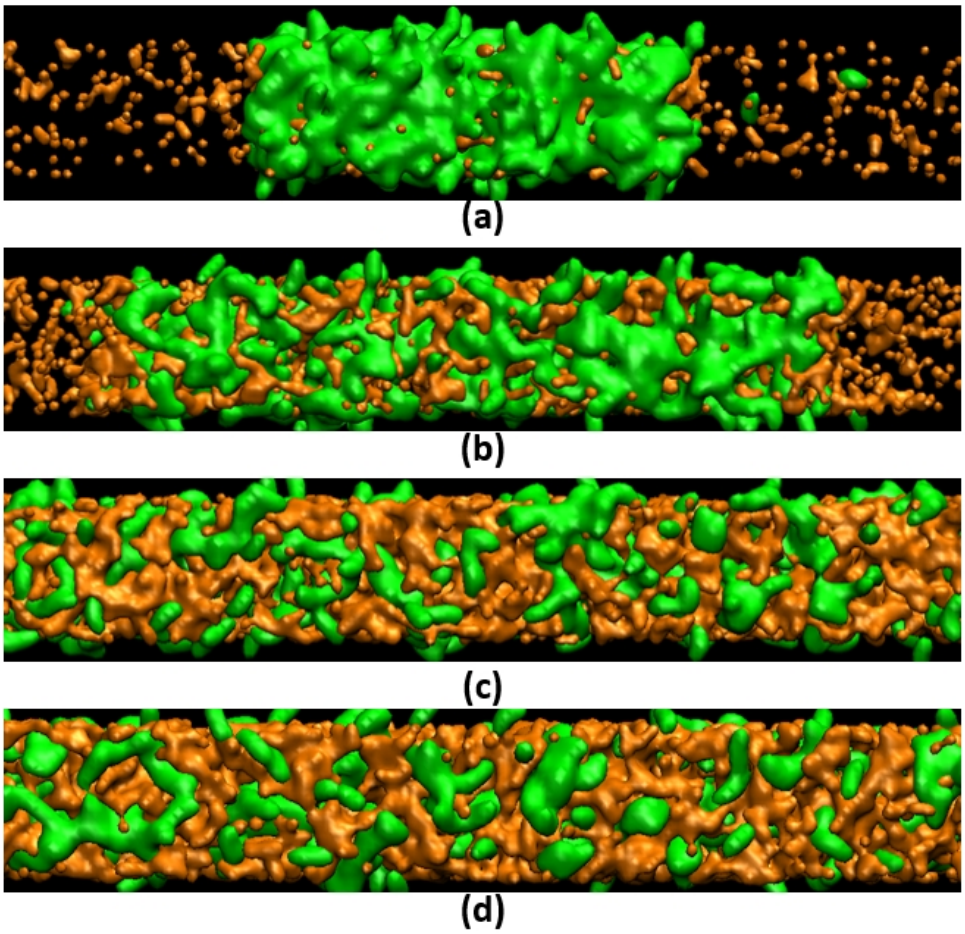


Figure 11. Distribution of decane and CO_2 clusters and the status of interfaces at (**a**) 4 MPa, (**b**) 8 MPa, (**c**) 16 MPa, and (**d**) 20 MPa. Clusters of decane molecules are colored in green, while those of CO_2 are colored in orange.

3.3. Determination of MMP Based on Intermolecular Interaction

The MMP reducer from the literature, C12PO6 [46], is used in this section to investigate the molecular scale boundary between miscibility and near miscibility. The interaction energies between the oil molecules are calculated for systems with and without MMP reducers, and the results are plotted in Figure 12. The interaction energy referred to in this manuscript is the sum of LJ (Lennard–Jones) and Coulombic energies. While the LJ energies are negative, indicating attraction between components, the coulombic energies are increasingly positive at higher pressures when the molecules are pressed closer to each other. This renders the transition of the interaction energies from negative to positive values, which is in line with an MD study by Zhang et al. [35]. As can be seen, curves for the system without any MMP reducers and the one with C12PO6 follow the same pattern. The interaction energy between the molecules first increases linearly with the increase in pressure. Then, the curves experience a decrease in the slope and further increase with the pressure, also in a linear manner before they eventually stabilize at relatively close values at approximately 7000 kJ/mol beyond 16 MPa. The physical meaning for the leveled-off stage is that the tendency of decane molecules to repel each other no longer increases with additional increases in pressure. In other words, the mixing of the decane and CO_2 molecules reaches an equilibrated state regardless of the pressure. This falls in line with the definition of miscibility. Additional interaction energies are calculated for different types of MMP reducers constructed as shown in Figure 4, and the results are included in Figure 12. The results indicate that in terms of the interaction energy, the interaction energies in the

presence of all constructed MMP reducers (other than C12PO6) are similar to that of a pure oil/CO_2 system. In other words, they do not effectively reduce the MMP. This is possibly due to there being only one O-containing functional group in their molecular structures, which provides minimal attraction to CO_2 molecules. It needs to be noted that although the IFT-based estimation method can to some extent predict MMP values from a recovery perspective, it can become invalid when a clearly defined interface region disappears, especially when cross-boundary components such as surfactants are distributed throughout the system. Alternatively, the interaction energy-based method does not yield results that match experimental values but rather reveals the true-miscibility range from a physical perspective, which, as will be demonstrated in a later section, can be used to compare the relative effectiveness in MMP reduction.

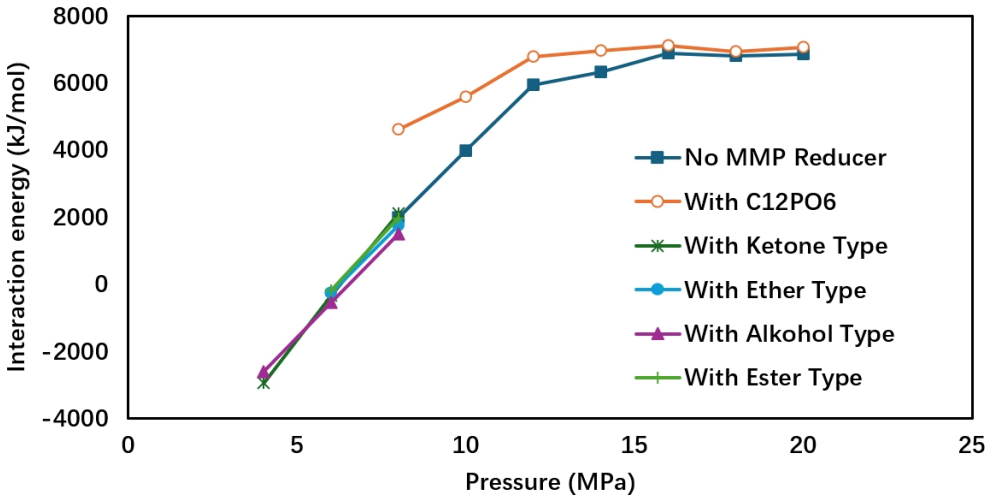


Figure 12. Interaction energies between decane molecules at different pressures in the absence and presence of MMP reducers.

This can be confirmed from the simulation trajectory as well; above 16 MPa, all the oil molecules are separated by CO_2 molecules and no micro-clusters exist. It is therefore an even mixing between molecules of different types. This will hereafter be referred to as the true-miscible stage, whereas the region with a medium slope (from 12 MPa to 16 MPa) is the near-miscible stage. During the near-miscible stage, the micro-clusters of oil molecules gradually become invaded and broken by CO_2 molecules that are essentially being squeezed into the oil clusters due to increasing pressure. This can be demonstrated by the rdf analysis of decane molecules during the simulation. Figure 13 shows the first peak of each individual decane rdf curves at different pressures in the absence and presence of the MMP reducer. As can be seen from Figure 13a,b, regardless of the presence of MMP reducers, with the increase in the pressure, the distribution of decane molecules experience a drastic change until 12 MPa, after which the changes are no longer significant. To better illustrate the change pattern, the peak values are plotted against the pressures and are shown in Figure 14, from which three stages can be identified. From 8 MPa to 12 MPa, the decrease in decane molecules around themselves exhibits a fast decline, indicating the breakage of the continuous oil phase into small aggregates (clusters). Between 12 MPa and 16 MPa, the decrease in the peak value experiences a mild drop, signifying the further collapsing of the oil clusters. And after 16 MPa, no significant change in the number density peak value can be observed, hinting that all decane molecules are at stable distribution regardless of the additional pressure.

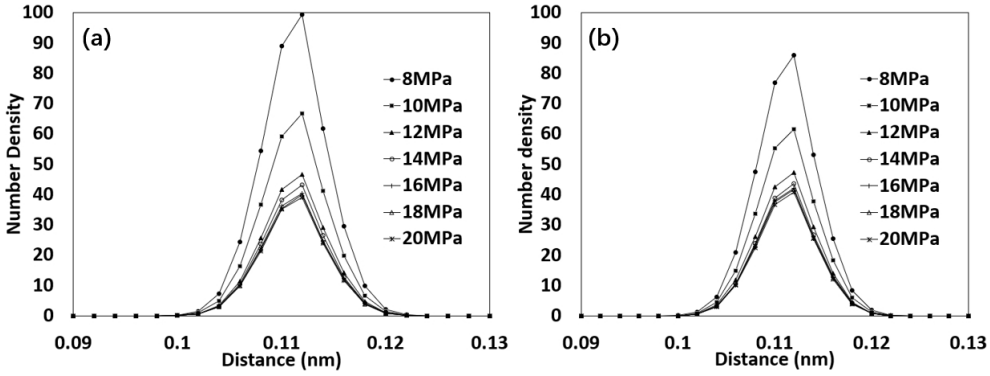


Figure 13. First peak of the RDF curves of decane molecules around themselves for (**a**) a binary system with just CO_2 and decane and (**b**) a CO_2-decane system in the presence of a C12PO6 MMP reducer.

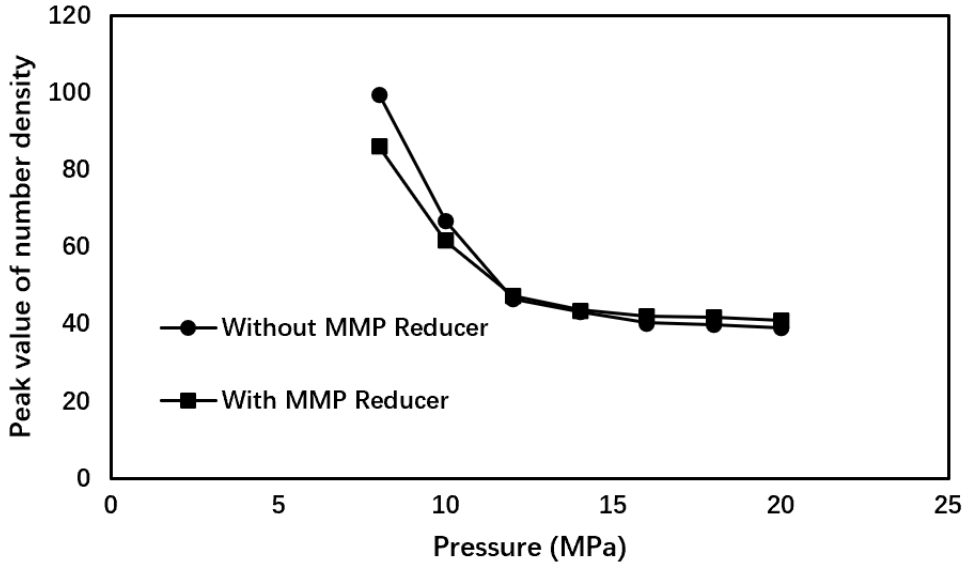


Figure 14. Peak values on the RDF curves for decane molecules around themselves in the presence and absence of MMP reducers.

If defined in this way, the minimum miscible pressure seems to stay the same in the presence and absence of the MMP reducer (Figure 12, both at 16 MPa). However, it can also be clearly seen from Figure 12 that despite the similarity in shape, the curves in the presence of MMP reducer appear more compressed in the y axis. The interaction energy between the oil molecules does not vary too much between the near-miscible stage and the true-miscible stage. On the contrary, for the system with just pure CO_2 and decane molecules, the interaction energy between oil molecules experience a larger extent of change between the near-miscible and true-miscible stages. Take the pressure of 12 MPa as an example. At such pressure, in the presence of MMP reducer, the binary system exhibits intermolecular energies that are almost similar to those in the true-miscible stage. However, the same cannot be said for the system without an MMP reducer, where the interaction energy between oil molecules may stand too far removed from what is required for the true-miscibility stage. This reveals the real function of MMP reducers. That is, they do not reduce the minimum miscible pressure but instead draw the near-miscibility stage sufficiently close to the true-miscibility stage, energy-wise, so that the system appears to have reached miscibility at a lower threshold pressure.

To recount, for the CO_2-decane systems in study, the non-miscible stage falls below the pressure of 12 MPa, during which the continuous oil phase gradually collapses into micro-clusters by dissolved CO_2 with increasing pressure. The near-miscible stage ranges from 12 to 16 MPa, during which the micro-clusters of decane molecules become further

invaded by CO_2 with increasing pressure, before the true-miscible stage is reached beyond 16 MPa when all molecules exhibit as a homogeneous mixture. The boundaries between the three stages is then made clear. The start of the near-miscible stage also marks the transition of any CO_2 in the oil phase from just being dissolved to being miscible.

4. Conclusions

To investigate the nature of near-miscible stage during CO_2 flooding and the role MMP reducers play during the process, the molecular dynamics approach was adopted to simulate the mixing between CO_2 and oil molecules. The following conclusions can be drawn from this work.

- Molecular dynamics simulations confirm the existence of a transition stage between non-miscibility and true miscibiltiy.
- The interfacial tension criterion is invalid for molecular dynamics approach to determine the MMP; rather, the interaction energy between oil molecules is a better parameter that clearly shows the boundary between non-miscibility, near miscibility, and true miscibility.
- For the non-miscible stage, the oil molecules collapse from a continuous phase into micro-clusters by disolved CO_2, while for the near-miscible stage, the micro-clusters are further broken by CO_2 molecules with increasing pressure, until the system reach the true-miscible stage, which is a monogeneous mixture.
- The MMP reducers do not really reduce the MMP; rather, they bring the near-miscibility stage close to the true-miscible stage in terms of energy, facilitating the mixing between CO_2 and the oil molecules.

The results obtained in this work provide a molecular-level understanding of the distinction between miscibility and near miscibility, and provide a theoretical criterion for the selection and designing of MMP reducers that can facilitate the application of the miscible flooding enhanced oil recover method. It should be noted that the role of different functional groups in enhancing the mixing of CO_2 and the oil phase was not sufficiently investigated in this work, and the interaction energy-based near-miscibility criterion was solely deduced upon the oxyethylene-type nonionic surfactant. Future work should expand the selection of surfactants and other MMP reducer types and further develop the structure–efficiency relationship for more efficient MMP reducer selection and design. The composition of the oil phase should also be more comprehensive to include the aromatics and other non-alkane components usually seen in crude oils.

Supplementary Materials: The following supporting information can be downloaded at: https://www.mdpi.com/article/10.3390/pr13020535/s1.

Author Contributions: Conceptualization, F.L., S.Z. and J.Z.; methodology, Z.L.; software, S.B.; validation, Y.C.; writing—original draft preparation, S.B.; writing—review and editing, F.L. All authors have read and agreed to the published version of the manuscript.

Funding: This research was funded by Basic Scientific Research Fund of Xinjiang Uyghur Autonomous Region (XQZX20220094) and the Tianchi Talent Project.

Data Availability Statement: The sample data files presented in this study are included in the supplementary material. Further inquiries can be directed to the corresponding author.

Acknowledgments: The authors gratefully acknowledge Liu Hongxian for his help in differentiating between miscibility and near miscibility.

Conflicts of Interest: Authors Feng Liu, Shengbing Zhang, Jiale Zhang, Zhaolong Liu, Yonghui Chen were employed by the PetroChina Tuha Oilfield Company. The remaining author declare that the research was conducted in the absence of any commercial or financial relationships that could be

construed as a potential conflict of interest. The company had no role in the design of the study; in the collection, analyses, or interpretation of data; in the writing of the manuscript, or in the decision to publish the results.

Abbreviations

The following abbreviations are used in this manuscript:

MMP	Minimum miscible pressure
PME	Particle Mesh Ewald
CHARMM	Chemistry at HARvard Macromolecular Mechanics
EMP	Elementary physical model
LJ	Lennard–Jones
IFT	Interfacial tension
RDF	Radial distribution function

References

1. Turkmenoglu, A.; Onel, S. Chemical assisted reduction on minimum miscibility pressure of viscouscrude oils. *Fuel* **2024**, *379*, 133006. [CrossRef]
2. Cui, W.; Liang, Y.; Masuda, Y.; Tsuji, T.; Matsuoka, T.; Takahashi, H. Estimation of the minimum miscibility pressure for CO_2-crude-oilsystems by molecular dynamics simulation. *Pet. Res.* **2023**, *8*, 1–10. [CrossRef]
3. Wang, Z.; Zhu, J.; Li, S. Novel strategy for reducing the minimum miscible pressure in a CO_2–oil system using nonionic surfactant: Insights from molecular dynamics simulations. *Appl. Energy* **2023**, *352*, 121966. [CrossRef]
4. Yang, Y.; Zhang, S.; Cao, X.; Lyu, Q.; Lyu, G.; Zhang, C.; Li, Z.; Zhang, D.; Zheng, W. CO_2 high-pressure miscible flooding and storage technology and its application in Shengli Oilfield, China. *Pet. Explor. Dev.* **2024**, *51*, 1247–1260. [CrossRef]
5. Meng, L.; Ge, M.; Liu, S.; Liu, X.; Fang, T. Molecular insight into the interfacial microstructural and miscible behavior of CO_2 flooding in tight reservoir. *Colloids Surf. A* **2025**, *705*, 135556. [CrossRef]
6. Zhu, Q.; Wu, K.; Guo, S.; Peng, F.; Zhang, S.; Jiang, L.; Li, J.; Feng, D.; Zhang, Y.; Chen, Z. Pore-scale investigation of CO_2-oil miscible flooding in tight reservoir. *Appl. Energy* **2024**, *368*, 123439. [CrossRef]
7. Wang, T.; Wang, L.; Meng, X.; Chen, Y.; Song, W.; Yuan, C. Key parameters and dominant EOR mechanism of CO_2 miscible flooding applied in low-permeability oil reservoirs. *Geoenergy Sci. Eng.* **2024**, *225*, 211724. [CrossRef]
8. Thomas, F.B.; Holowach, N.; Zhou, X.; Bennion, D.B.; Bennion, D.W. Miscible or near-miscible gas injection, which is better? In Proceedings of the SPE/DOE Improved Oil Recovery Symposium, Tulsa, OK, USA, 16–18 April 1994; Society of Petroleum Engineers: Richardson, TX, USA, 1994. [CrossRef]
9. Franklin M.; Orr, J.; Jensen, C.M. Interpretation of pressure-composition phase diagrams for CO_2 crude-oil systems. *SPE J.* **1984**, *24*, 485–497. [CrossRef]
10. Orr, F.M., Jr.; Silva, M.K. Equilibrium phase compositions of CO_2 hydrocarbon mixtures-part 1. *SPE J.* **1983**, *23*, 272–280. [CrossRef]
11. Zick, A.A. A combined condensing-vaporizing mechanism in the displacement of oil by enriched gases. In Proceedings of the SPE Annual Technical Conference and Exhibition, New Orleans, LA, USA, 5–8 October 1986; Society of Petroleum Engineers: Richardson, TX, USA, 1986. [CrossRef]
12. Stalkup, F. Carbon dioxide miscible flooding: Past, Present, and outlook for the future. *J. Pet. Technol.* **1978**, *30*, 1102–1112. [CrossRef]
13. Novosad, Z. On the aspects of reservoir fluids phase behavior important in design of miscible gas injection processes. In Proceedings of the IOR 1991—6th European Symposium on Improved Oil Recovery, Stavanger, Norway, 21–23 May 1991; European Association of Geoscientists & Engineers: Utrecht, The Netherlands, 1991. [CrossRef]
14. Shyeh-Yung, J.J.; Stadler, M.P. Effect of injectant composition and pressure on displacement of oil by enriched hydrocarbon gases. *SPE Res. Eng.* **1995**, *10*, 109–115. [CrossRef]
15. Grigg, R.B.; Gregory, M.D.; Purkaple, J.D. The effect of pressure on improved oilflood recovery from tertiary gas injection. *SPE Res. Eng.* **1997**, *12*, 179–188. [CrossRef]
16. Schechter, D.S.; Grigg, R.; Guo, B.; Schneider, B. Wellman unit CO_2 flood: Reservoir pressure reduction and flooding the water oil. In Proceedings of the SPE Annual Technical Conference and Exhibition, New Orleans, LA, USA, 27–30 September 1998; Society of Petroleum Engineers: Richardson, TX, USA, 1998. [CrossRef]
17. Dong, M.; Huang, S.; Srivastava, R. Effect of solution gas in oil on CO_2 minimum miscibility pressure. *J. Can. Pet. Technol.* **2000**, *39*, *53–61*. [CrossRef]

18. Chen, H.; Zhang, X.; Chen, Y.; Tang, H.; Mei, Y.; Li, B.; Shen, X. Study on pressure interval of near-miscible flooding by production gas Re-injection in QHD offshore oilfield. *J. Pet. Sci. Eng.* **2017**, *157*, 340–348. [CrossRef]
19. dos Santos Bastos, L.; da Silva Lins, I.E.; de Tarso Vieira e Rosa, P.; Costa, G.M.N.; de Melo, S.A.B.V. An experimental assessment of seawater alternating near-miscible CO_2 for EOR in pre-salt carbonate reservoirs. *Geoenergy Sci. Eng.* **2023**, *230*, 212227. [CrossRef]
20. Yu, H.; Lu, X.; Fu, W.; Wang, Y.; Xu, H.; Xie, Q.; Qu, X.; Lu, J. Determination of minimum near miscible pressure region during CO_2 and associated gas injection for tight oil reservoir in Ordos Basin, China. *Fuel* **2020**, *263*, 116737. [CrossRef]
21. Alhosani, A.; Scanziani, A.; Lin, Q.; Pan, Z.; Bijeljic, B.; Blunt, M.J. In situ pore-scale analysis of oil recovery during three-phase near-miscible CO_2 injection in a water-wet carbonate rock. *Adv. Water Resour.* **2019**, *134*, 103432. [CrossRef]
22. Shyeh-Yung, J.G.J. Mechanisms of miscible oil recovery: Effects of pressure on miscible and near-miscible displacements of oil by carbon dioxide. In Proceedings of the SPE Annual Technical Conference and Exhibition, Dallas, TX, USA, 6–9 October 1991; Society of Petroleum Engineers: Richardson, TX, USA, 1991. [CrossRef]
23. Burger, J.E.; Springate, G.S.; Mohanty, K.K. Experiments on bypassing during gasfloods in heterogeneous porous media. *SPE Res. Eng.* **1996**, *11*, 109–115. [CrossRef]
24. Pingping, S.; Lei, H. Flow mechanisms of multi-phase multi-component CO_2-crude oil system in porous media. *Acta Pet. Sin.* **2009**, *30*, 247–251. (In Chinese)
25. Uleberg, K.; Hoier, L. Miscible Gas Injection in Fractured Reservoirs. In Proceedings of the SPE/DOE Improved Oil Recovery Symposium, Tulsa, OK, USA, 13–17 April 2002; Society of Petroleum Engineers: Richardson, TX, USA, 2002 ; number SPE-75136-MS. [CrossRef]
26. Bui, L.H.; Tsau, J.S.; Willhite, G.P. Laboratory investigations of CO_2 near miscible application in Arbuckle reservoir. In Proceedings of the SPE Improved Oil Recovery Symposium, Tulsa, OK, USA, 24–28 April 2010; Society of Petroleum Engineers: Richardson, TX, USA, 2010 ; number SPE-129710-MS. [CrossRef]
27. Parvazdavani, M.; Motahhari, S.M.; Ansari, V. Lab and field scale modeling of near miscible CO_2 injection in different porous mediums. *J. Pet. Technol.* **2015**, *5*, 53–68. [CrossRef]
28. Fang, T.; Zhang, Y.; Liu, J.; Ding, B.; Yan, Y.; Zhang, J. Molecular insight into the miscible mechanism of CO_2/C10 in bulk phase and nanoslits. *Int. J. Heat Mass Transf.* **2019**, *141*, 643–650. [CrossRef]
29. Alhosani, A.; Lin, Q.; Scanziani, A.; Andrews, E.; Zhang, K.; Bijeljic, B.; Blunt, M.J. Pore-scale characterization of carbon dioxide storage at immiscible and near-miscible conditions in altered-wettability reservoir rocks. *Int. J. Greenh. Gas Control* **2021**, *105*, 103232. [CrossRef]
30. Yuan, L.; Zhang, Y.; Liu, S.; Zhang, J.; Song, Y. Molecular dynamics simulation of CO_2-oil miscible fluid distribution and flow within nanopores. *J. Mol. Liq.* **2023**, *380*, 121769. [CrossRef]
31. Sun, Q.; Bhusal, A.; Zhang, N.; Adhikari, K. Molecular insight into minimum miscibility pressure estimation of shale oil/CO_2 in organic nanopores using CO_2 huff-n-puff. *Chem. Eng. Sci.* **2023**, *280*, 119024. [CrossRef]
32. Wang, X.; Li, S.; Tong, B.; Jiang, L.; Lv, P.; Zhang, Y. Wettability and capillary behavior in a CO_2–oil–solid system under near-miscible conditions: A pore-scale study. *Fuel* **2024**, *364*, 131164. [CrossRef]
33. Wang, G.; Pickup, G.; Sorbie, K.; Mackay, E.; Skauge, A. Numerical study of CO_2 injection and the role of viscous crossflow in near-miscible CO_2-WAG. *J. Nat. Gas Sci. Eng.* **2020**, *74*, 103112. [CrossRef]
34. Luo, Y.; Yang, S.; Zhang, Y.; Kou, G.; Zhao, S.; Zhao, X.; Zhang, X.; Chen, H.; Wang, X.; Xiaio, Z.; et al. Characteristics and Mechanisms of CO_2 Flooding with Varying Degrees of Miscibility in Reservoirs Composed of Low-Permeability Conglomerate Formations. *Processes* **2024**, *12*, 1203. [CrossRef]
35. Zhang, W.; Guo, P.; Jia, N.; Chen, F.; Liu, H.; Wang, Z.; Ge, X. The effects of nonionic surfactants on enhancing miscibility between oiland CO_2: A molecular dynamics study. *J. Mol. Liq.* **2024**, *408*, 125076. [CrossRef]
36. Dong, Z.; Qian, S.; Li, W.; Ma, X.; Hou, T.; Zhang, T.; Yang, Z.; Lin, K.; Yi, H. Molecular dynamics simulation of surfactant reducing MMP between CH4 and n-decane. *Heliyon* **2024**, *10*, e26441. [CrossRef] [PubMed]
37. Gong, H.; Zhang, H.; Lv, W.; Zhang, Z.; Sun, H.; Xu, L.; Dong, M. Impact of citrate ester surfactants on the MMP, extraction and swelling behaviors between CO_2 and oil: Applications for enhanced shale oil recovery. *Chem. Eng. Sci.* **2025**, *304*, 121039. [CrossRef]
38. Alzobaidia, S.; Lee, J.; Jiries, S.; Da, C.; Harris, J.; Keene, K.; Rodriguez, G.; Beckman, E.; Perry, R.; Johnston, K.P.; et al. Carbondioxide-in-oil emulsions stabilized with silicone-alkyl surfactants for waterless hydraulic fracturing. *J. Colloid Interface Sci.* **2018**, *526*, 253–267. [CrossRef] [PubMed]
39. Wang, Q.; Zhang, X.; Wang, W.; Zhao, H.; Liu, S.; Wang, H.; Han, F. Gas-liquid interface properties of fluorocarbon and hydrocarbon surfactants and their mixed foams: Molecular dynamics simulations and experimental studies. *J. Environ. Chem. Eng.* **2024**, *12*, 114685. [CrossRef]
40. Michel, A.; Brauch, H.J.; Worch, E.; Lange, F.T. Homologue specific analysis of a polyether trisiloxane surfactant in German surface waters and study on its hydrolysis. *Environ. Pollut.* **2024**, *186*, 126–135. [CrossRef] [PubMed]

41. Lindahl, E.; Hess, B.; van der Spoel, D. GROMACS 3.0: A package for molecular simulation and trajectory analysis. *J. Mol. Model.* **2001**, *7*, 306–317. [CrossRef]
42. Francis, M.G. The surface activity of polymers in cosolvated systems determined from computational simulation. *Polymer* **2016**, *82*, 133–137. [CrossRef]
43. Brooks, B.; Brooks, C.; MacKerell, A.; Nilsson, J.L.; Petrella, R.; Roux, B.; Won, Y.; Archontis, G.; Bartels, C.; Boresch, S.; et al. CHARMM: The biomolecular simulation program. *J. Comput. Chem.* **2009**, *30*, 1545–1614. [CrossRef]
44. Harris, J.G.; Yung, K.H. Carbon dioxide's liquid-vapor coexistence curve and critical properties as predicted by a simiple molecular model. *J. Phys. Chem.* **1995**, *99*, 12021–12024. [CrossRef]
45. Zhang, Y.; Feller, S.E.; Brooks, B.R.; Pastor, R.W. Computer simulation of liquid/liquid interfaces. I. Theory and application to octane/water. *J. Chem. Phys.* **1995**, *103*, 10252–10266. [CrossRef]
46. Xinle, M. Molecular Dynamics Simulation-Based Study on the Reduction of Miscible Pressure in CO_2 Displacement. Ph.D. Thesis, Xi'an Shiyou University, Xi'an, China, 2023. (In Chinese)
47. Chen, Z.; Chen, J.; Zhang, X. A comprehensive review of minimum miscibility pressure determinationand reduction strategies between CO_2 and crude oil in CCUS processes. *Fuel* **2024**, *384*, 134053. [CrossRef]

Disclaimer/Publisher's Note: The statements, opinions and data contained in all publications are solely those of the individual author(s) and contributor(s) and not of MDPI and/or the editor(s). MDPI and/or the editor(s) disclaim responsibility for any injury to people or property resulting from any ideas, methods, instructions or products referred to in the content.